BBA Advances 1 (2021) 100018

Contents lists available at ScienceDirect

BBA Advances

journal homepage: www.sciencedirect.com/journal/bba-advances

Effect of quercetin on lipid membrane rigidity: assessment by atomic force microscopy and molecular dynamics simulations

Jad Eid [a,b], Alia Jraij [a,*], Hélène Greige-Gerges [a], Luca Monticelli [b,*]

[a] Bioactive Molecules Research Laboratory, Doctoral School of Sciences and Technologies, Faculty of Sciences, Lebanese University, Lebanon
[b] Molecular Microbiology and Structural Biochemistry (MMSB), CNRS & Univ. Claude Bernard Lyon I, UMR 5086, Lyon F-69007, France

ARTICLE INFO

Keywords:
Quercetin
Lipoid E80
Young modulus
Area compressibility modulus
Molecular dynamics
AFM

ABSTRACT

Quercetin (3,3',4',5,7-pentahydroxyl-flavone) is a natural flavonoid with many valuable biological effects, but its solubility in water is low, posing major limitations in applications. Quercetin encapsulation in liposomes increases its bioavailability; the drug effect on liposome elastic properties is required for formulation development. Here, we quantify the effect of quercetin molecules on the rigidity of lipoid E80 liposomes using atomic force microscopy (AFM) and molecular dynamics (MD) simulations. AFM images show no effect of quercetin molecules on liposomes morphology and structure. However, AFM force curves suggest that quercetin softens lipid membranes; the Young modulus measured for liposomes encapsulating quercetin is smaller than that determined for blank liposomes. We then used MD simulations to interpret the effect of quercetin on membrane rigidity in terms of molecular interactions. The decrease in membrane rigidity was confirmed by the simulations, which also revealed that quercetin affects structural and dynamic properties: membrane thickness is decreased, acyl chains disorder is increased, and diffusion coefficients of lipid molecules are also increased. Such changes appear to be related to the preferential localization of quercetin within the membrane, near the interface between the hydrophobic core and polar head groups of the lipids.

Introduction

Quercetin (3,3',4',5,7-pentahydroxyl-flavone) is a common flavonoid occurring naturally in a variety of brightly colored plant-based foods (e.g., onion, apple, broccoli, tea, and red wine [1]). Quercetin has been the subject of many investigations because of its numerous beneficial properties, including antioxidant [1,2], antiviral [3,4], anticancer [5], antimicrobial [6,7], anti-inflammatory [8,9], and anti-obesity [10] properties. Currently there is growing interest for using quercetin as an ingredient in pharmaceutical preparations or food products. However, because of its low aqueous solubility (about 0.01 mg/mL at 25 °C) [11], low bioavailability [12], and reduced chemical stability [11], the use of quercetin is still limited. The encapsulation of quercetin in liposomes could overcome the drawbacks related to the physico-chemical properties of this flavonoid [13–15]. Experimental works show that quercetin can be incorporated into liposomes [15,16]. When encapsulating drugs or other small molecules, it is important that liposome mechanical stability and elastic properties are preserved, since liposome elasticity impacts size, shape, membrane permeability, and drug loading efficiency [17–20], and tissue targeting [17,21]. These aspects have been investigated by several research teams [4,18,22–24]. Liposome elasticity may be affected by the incorporation of quercetin, but the effect of quercetin on liposome's elasticity is still not known.

Here, we aim to characterize the elastic properties of liposomes encapsulating quercetin. To this end, we use both experimental and computational methods. We are particularly interested in characterizing the elasticity of nano-sized liposomes, with size below 100 nm, because they are the most useful for drug delivery purposes. Considering the small size, Atomic Force Microscopy (AFM) is a good choice for experimental measures of elasticity, as it can be used directly on nano-sized liposomes without additives. AFM can provide high-resolution images of a surface at nanometer scales, and it has been often used in the study of lipid vesicles [25–27]. Recently, we optimized the AFM experimental conditions for measuring the Young modulus of lipoid E80 vesicles [28]. The optimized conditions are applied in the present study. As for the choice of liposome composition, we demonstrated in a previous study that quercetin-loaded lipoid E80 liposomes exhibited better encapsulation efficiency compared to Phospholipon 90H and Lipoid S100 liposomes formulations [18]. Taking into consideration the yield of the encapsulation process, we use Lipoid E80 as the formulation of choice in

* Corresponding authors.
E-mail addresses: ajraij@ul.edu.lb (A. Jraij), luca.monticelli@inserm.fr (L. Monticelli).

https://doi.org/10.1016/j.bbadva.2021.100018

Available online 25 June 2021

the present study. We then interpret the AFM data using molecular dynamics (MD) simulations at the atomistic level, mimicking experimental conditions as closely as possible. Previous MD investigations probed the position and orientation of quercetin in lipid membranes, and showed that quercetin is found about half way between the hydrophobic core and the polar head groups [29–31]. Here, we use MD simulations to predict the effect of quercetin on membrane elastic properties, and particularly the area compressibility modulus. In addition, we use simulations to provide a detailed view of the structure and dynamics of bilayers incorporating quercetin, allowing for an interpretation of the experimental findings in terms of interactions at the atomic level.

Materials and methods

Experimental materials

Lipoid E80, purchased from Lipoid GmbH (Ludwigshafen, Germany) is constituted of 80-86% egg phosphatidylcholine (PC), 7-9.5% phosphatidylethanolamine (PE), 3% lyso-PC, 0.5% lyso-PE, 1-2% sphingomyelin, 2% water, 0.2% ethanol. Ethanol, quercetin (>95%), and cholesterol (95%) (Chol) were purchased from Sigma Aldrich (France).

Pyrex-nitride probes triangular cantilevers PNP-TR (NanoWord Innovative Technologies, Nano and More, Paris, France) integrating a sharpened pyramidal tip with a radius < 10 nm and a macroscopic half cone 35^{o} angle, were used for imaging and indenting liposomes. Mica sheets (9 mm diameter and 0.1 mm thickness) were purchased from Nano and More (France).

Experimental setup: preparation of liposomes

The ethanol injection method was used to prepare liposomes according to the protocol described by Azzi et al. [18]. Two batches were prepared: 1, lipoid E80:Chol liposomes; 2, quercetin loaded lipoid E80:Chol liposomes. Briefly, the appropriate amounts of phospholipids, Chol, and quercetin, were dissolved in ethanol (10 ml) at concentrations of 40, 20, and 3.02 mg/ml, respectively. The lipoid E80:Chol molar ratio was of 100:98 and that of lipoid E80:Chol:quercetin was of 100:98:20. The organic solution was then injected, using a syringe pump into ultra-pure water (20 ml) under magnetic stirring (400 rpm). Ethanol was removed by rotary evaporation at 40°C under reduced pressure and the liposome suspensions were stored at 4°C. AFM measurements were realized during three months after the preparation of liposomes. The final composition was 100:74 (phospholipids:Chol) for blank liposomes and 100:55:15 (phospholids:Chol:quercetin) for quercetin-loaded liposomes.

AFM measurements

AFM imaging and force measurements were performed at room temperature using an Agilent 5420 microscope (Key sight, California, USA) equipped with the AFM probe described before. An aliquot of the liposomal suspension was diluted 10 times in ultrapure water. Then, 10 µl of the diluted formulation was deposited on freshly cleaved mica surface and left for 15 min in air at room temperature, for adsorption. The mica sheet was rinsed with ultrapure water to remove the non-adsorbed vesicles. The sample was then imaged in contact mode with a typical scan rate of 1 Hz, resolution of 512 × 512 pixels per image, 5 × 5, and 2 × 2 µm^2 images sizes, scanning angle of 0^0, and a set point typically below 0.1 nN. For each sample, adsorbed vesicles were observed, and 200 force curves were recorded for 200 different liposomes (one curve per liposome), in force spectroscopy mode. Each curve was obtained by indenting centrally an adsorbed vesicle with a maximum force of 1.5 nN and a rate of 0.145 µm/s. Before the indentation measurement, the deflection sensitivity (deflection/voltage ratio) was calibrated on a clean mica surface. The force calibration plot was converted into force versus liposome deformation. This is possible by determining the zero force point, and the zero separation point Z_0 between the tip and the sample. Zero force was determined where the separation tip-sample is large enough and the cantilever deflection attains its constant initial value d_0. Z_0 was identified where the deflection of the cantilever was linear with the expansion of the piezo scanner.

In our previous work, we demonstrated that Shell model provides the closest agreement between our AFM data and other experimental data for the membrane bending modulus comparing to Hertz model [28]. Hence, we fitted the force versus liposome deformation curves with Shell model to extract the Young modulus E. The model was applied in the elastic region, when the indentation of the vesicle did not exceed 10% of its diameter. The Young modulus (E) was then determined using the following relationship, linking the measured force (F) with the measured deformation (δ) [32]:

$$F = \frac{E4h^2\ C}{R\sqrt{3(1-\upsilon^2)}}\delta \tag{1}$$

where R is the radius of curvature of the indented liposomes, and h is the membrane thickness. C is a correction factor introduced by Berry *et al.* for adsorbed vesicles on a rigid substrate [33]. The authors suggest that the measured indentation is the sum of indentions caused by both the indenter and the substrate [33]. The Poisson's ratio (υ) is assumed to be 0.5 and the membrane thickness 4 nm.

The bending modulus k_c can, in principle, be derived from the following relation [34]:

$$k_c = \frac{Eh^3}{12(1-\upsilon^2)} \tag{2}$$

Molecular simulations

We built the topology for quercetin using an automatic server, the LigParGen web-based service [35–37], providing a complete topology for the OPLS-AA force field [38], compatible with the GROMACS software [39] that we used for all simulations. We used only the neutral form of the molecule, because the pK_a of quercetin is close to neutral pH [40]; also, we are mostly interested in studying the molecule in a membrane environment, where the pK_a will be higher, i.e., it will be more difficult to deprotonate the weak acid and the neutral form will be more likely [40]. The LigParGen server produces partial charges based on the precise geometry of the submitted molecule, so we used 2 conformations for quercetin, differing by the rotation of the main dihedral angle, corresponding to conformations (a) with the rings in the same plane and (b) rotated by 180 degrees. The partial charges produced by the server were similar but not identical, and we used the average value of the partial charge for each atom. The complete topology is provided in Supporting Information. Fig. 1, show the geometry of quercetin

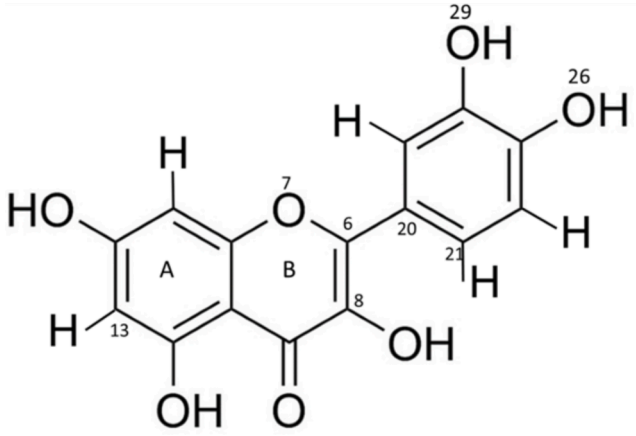

Fig. 1. Geometry and atom numbering of quercetin.

molecule.

We then set up a simulation of one quercetin molecule in a box full of SPC (single point charge) water [41] of size 4 × 4 × 4 nm. We first performed energy minimization (steepest descent, 10000 steps), then equilibration for 20 ns in the NPT ensemble (298K and 1 bar), and finally a production run for 200 ns.

We used model membranes similar to the ones used in the AFM experiments, at the same temperature, to mimic AFM experimental conditions. We used the MemGen [42] software to generate starting structures for lipid bilayers, containing 138 lipid molecules (80 POPC, 10 POPE, and 48 Chol molecules) in a box full of water (4373 water molecules) with initial dimension of $x = 5.9\ nm$, $y = 5.9\ nm$, *and* $z = 8\ nm$.

We used the force field by Berger for phospholipids [43], compatible with OPLS-AA [44,45] (used for quercetin molecules and cholesterol). The reliability of the Berger force field has been demonstrated in a number of previous works on the partitioning of small molecules in lipid membranes [44–46].

The Lennard-Jones and Coulomb interactions were cut off at 1.2 nm (r_{cut}), with the potentials shifted to zero at the cut off. The Lennard–Jones potential was shifted from $r_{shift} = 1\ nm$ to r_{cut}, while electrostatic interactions were shifted from $r_{shift} = 1\ nm$ to r_{cut}. A relative dielectric constant $\varepsilon = 1$ was used for explicit screening. Long-range electrostatic interactions were calculated with the Particle-Mesh Ewald (*PME*) algorithm [47,48], with Fourier spacing set to 0.12 and the interpolation order (pme-order) set to 1.

Membrane systems were first energy minimized (steepest descent method, 10000 steps), then equilibrated for 20 *ns* in the isothermic-isobaric ensemble (*NPT*), with the temperature set to 298 *K* and the pressure (*P*) to 1 *bar*. After equilibration, we generated five systems with different quercetin concentration, containing 0, 4, 8, 12, and 16 quercetin molecules. Quercetin molecules were inserted in the membrane in a symmetric fashion, with the same number of molecules in both leaflets. The initial orientation of quercetin was with the aromatic rings parallel to the membrane normal, and the phenyl group closer to the water region. Then, we minimized the energy and equilibrated each system in the isothermal-isobaric (*NPT*) ensemble for 20 *ns*, with the temperature $T = 298\ K$ and $P = 1\ bar$. Production runs were carried out for 900 *ns*.

We performed all molecular dynamics simulations using the GROMACS software (v. 2016.4) [39]. In all simulations we used the leap-frog algorithm for the integration of the equation of motion, with an integration time step of 2 *fs* in conjunction with the *LINCS* algorithm [49] to constrain the bonds involving hydrogen atoms. To maintain constant temperature, we used the Bussi-Donadio-Parrinello thermostat (named v-rescale in Gromacs [50]), with a time constant of 1 *ps* and a reference temperature of 298 *K*. For pressure coupling, we used Berendsen [51] and Parinello-Rahman [52] method in equilibration and production run, respectively, with semi-isotropic coupling type, time constant of 10 *ps*, and a compressibility of 4.5×10^{-5}.

All analyses were performed over the last 800 *ns* of simulation. We estimated the area per lipid (A_l) in the simulations from the total number of lipids per leaflet and the area of the membrane projected in the *xy* plane (obtained from the box dimensions), using the following equation:

$$A_l = \frac{2 \times L_x \times L_y}{n_{lipids}} \tag{3}$$

L_x, L_y are respectively the *x* and *y* dimensions of the simulation box, and n_{lipids} represents the number of lipids in the system. Statistical uncertainties were calculated using the GROMACS tool gmx analysis.

We calculated the membrane thickness as the difference between the average position (along the bilayer normal, i.e., the *z* axis) of the phosphorous atoms in the lipids head groups. The latter was calculated using the GROMACS tool gmx density. The statistical uncertainty was estimated using block averaging, by dividing the simulation into 10 equal blocks and computing the difference between the highest and lowest values. This method is justified by the small size of the bilayers, leading to negligible undulations.

We calculated the angular distribution defined by the bilayer normal ($z-axis$) and the normal vector of the plane defined by the atoms 6, 8 and 13 of quercetin molecule using the GROMACS tool gmx gangle. The order parameter of C-H bonds in lipid bilayers was calculated (using the GROMACS tool gmx order) as:

$$S_{CH} = \frac{1}{2}\left\langle 3cos^2\theta - 1 \right\rangle \tag{4}$$

where θ is the angle between the C−H bond vector and the bilayer normal, and angular brackets indicate ensemble and time averages.

The lateral diffusion coefficient, *D*, of POPC lipids was calculated using the Einstein relation, from the mean square displacement (MSD) versus time, using the GROMACS module gmx msd. The MSD was calculated for the phosphorus atoms, and least-squares fitted to a straight line ($4Dt + c$), where *t* is time and *c* is a fitting constant. Uncertainties were estimated using block averaging; we split the production run in two equal blocks, and the difference between average values was used as an estimate of the statistical uncertainty.

The isothermal compressibility modulus K_A was calculated from area fluctuations:

$$K_A = k_B T \frac{A_0}{< (A - A_0)^2 >} \tag{5}$$

where k_B is Boltzmann constant, *T* is the simulation temperature in Kelvin, A_0 is the average in-plane area of the membrane and *A* is the instantaneous in-plane area. Statistical uncertainties were estimated from block averaging.

Results and discussion

AFM imaging and measurements

We prepared samples containing lipids and quercetin as detailed in Methods, then used AFM in contact mode to visualize the adsorbed vesicles on the mica substrate. Fig. 2 shows blank Lipoid E80 liposomes and Lipoid E80 liposomes loaded with quercetin, adsorbed on a clean mica sheets.

The presence of quercetin did not affect the morphology of the liposomes. For both blank and quercetin-loaded liposomes, we found an heterogeneous distribution of sizes, ranging from 50 *to* 200 *nm*, and the same mean height of 22 ± 3 *nm*. Liposomes showed a mean size of 98 ± 15 *nm* for blank liposomes and 105 ± 20 *nm* for quercetin loaded liposomes. These distributions were confirmed by laser granulometry analysis (data not shown), and are in agreement with those obtained by Azzi et al. for Lipoid E80 liposomes containing cholesterol [18].

We used AFM to reveal the effect of quercetin on the liposome rigidity. Adsorbed vesicles from both samples were indented on a fix point on their upper surface, using a relatively small force, to avoid vesicle damage. We indented 200 liposomes from each sample, determined force vs deformation curves, and calculated the Young modulus from each curve (i.e., for each vesicle) as the slope of the force vs deformation curve in the elastic region (from 0 to 2.2 *nm*, see Fig. 3). We only collected the data on the elastic behavior when the degree of deformation of liposomes was small, i.e., the maximum indentation was about 10% of the measured liposome height. The curves were fitted using the modified Shell model (see Methods).

As the example shows (Fig. 3), steeper force-deformation curves were generally obtained for blank liposomes, indicating that quercetin softens lipid membranes. Averaging over 200 vesicles for each composition, we obtained a value of 22 ± 5 *MPa* for the Young modulus of blank liposomes, and 15 ± 4 *MPa* for quercetin-loaded liposomes. These correspond to bending moduli of 38 ± 7 k_BT and 26 ± 6 k_BT

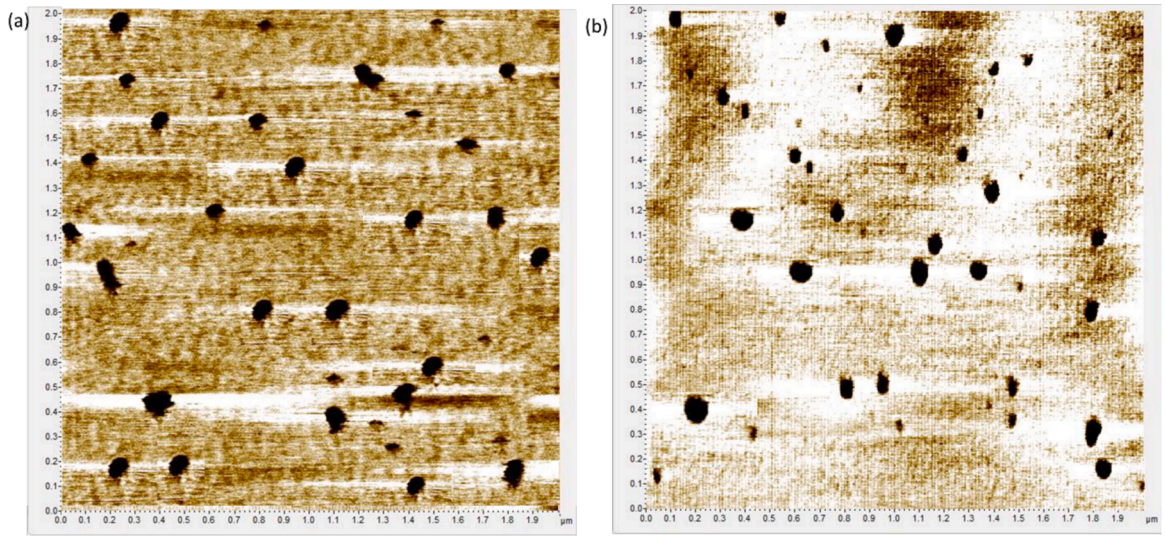

Fig. 2. AFM 2 × 2 μm^2images of (a) blank Lipoid E80 liposomes and (b) quercetin-loaded Lipoid E80 liposomes, adsorbed on mica substrate

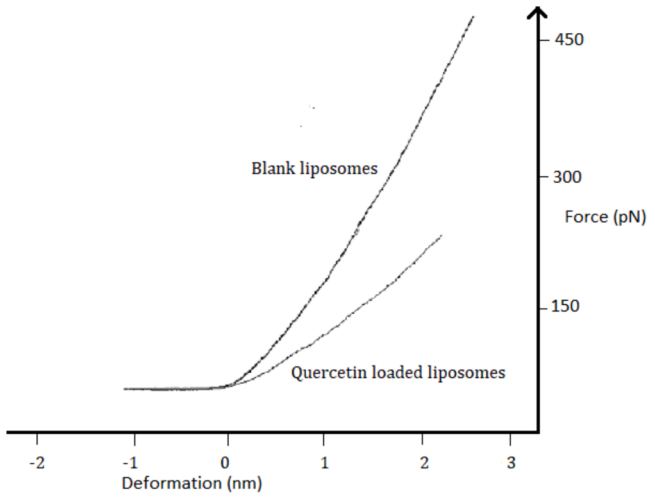

Fig. 3. Force-deformation curves, in the elastic region, obtained for blank and quercetin loaded lipoid E80 liposomes, during the approach of the tip to the sample.

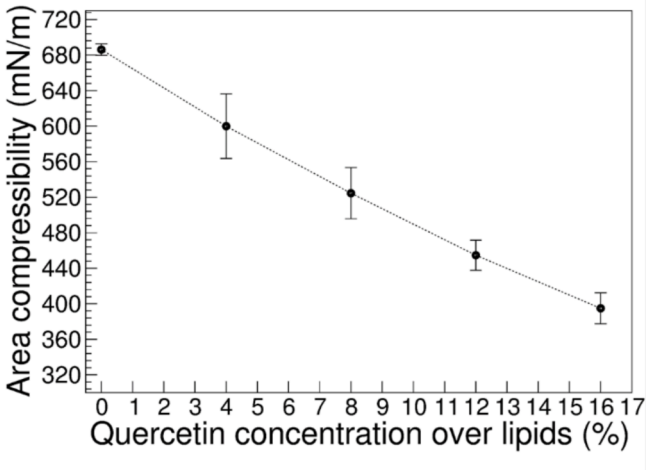

Fig. 4. Area compressibility modulus of lipid membranes POPC+POPE: cholesterol:quercetin as a function of quercetin concentration (reported as molar fraction of quercetin over lipids).

for blank and quercetin-loaded liposomes, respectively (obtained from Eq. (2)). The bending modulus of blank liposomes (lipoid E80:Chol 100:74) is in reasonable agreement with previously reported values obtained via AFM by Takechi-Haraya et al. [53] on EggPC liposomes, containing cholesterol with molar ratio 50:50 (31.64 k_BT). The difference between bending moduli is around 16% and may be explained by the difference in cholesterol concentration (100:74 in our sample vs 50:50 in ref. 52), the AFM probe characteristics (cantilever force constant 0.08 *vs* 0.15 *N/m*, and tip radius 10 *vs* 20 *nm*), and the mathematical model (modified Shell vs Shell).

The reduction in elastic modulus in the system containing quercetin appears to be due to the presence of quercetin, and to the difference in cholesterol concentration (42 vs 32% in blank and quercetin-loaded liposomes, respectively). We remark here that the initial concentration of cholesterol in both systems (blank and quercetin loaded liposomes) during the preparation of liposomes was the same (20 mg/ml see paragraph 2.1), while the incorporation rate of cholesterol in liposomes was different in the two systems [18]. Due to differential incorporation of cholesterol, it is not clear to what extent the reduction in the elastic moduli should be ascribed to quercetin. Moreover, available experimental data does not allow to interpret the decrease in bending rigidity in terms of molecular structures and interactions, and how they change in the presence of quercetin. Such molecular interpretation can be afforded by MD simulations.

MD simulations

We used MD simulations at the atomistic level to understand the effect of quercetin on the properties of ternary lipid mixtures consisting of POPC:POPE:Chol. We simulated such ternary lipid mixtures in the presence of different concentrations of quercetin, from 4% to 16 % (molar fraction over phospholipids). We used the simulations to characterize membrane elastic properties by calculating the area compressibility modulus (K_A). This is linked to the other elastic moduli of bilayer membranes [54], although not directly comparable to the Young modulus measured experimentally by AFM. First, we calculated the value of K_A in the absence of quercetin, and compared it with values reported in the literature for similar membranes (see Table 1).

Our value of area compressibility modulus is in reasonable agreement with values previously obtained via simulations by Docktorova *et al.* for POPC:Chol (70:30) [55] using both box area fluctuation methods and local thickness fluctuations (see Table 1), and those

Table 1
Values of area compressibility modulus determined in literature and in the present work for membranes containing POPC and Chol.

Bilayer	Molar ratio (lipid:Chol)	K_A (mN/m)	Temperature (K)	Method	Reference
POPC:ChoL	70:30	562 ± 87	288	Box area fluctuation (CHARMM36)	[55]
		757 ± 87	288	Local thickness fluctuations (LTF) (CHARMM36)	
POPC+POPE:ChoL	70:30	401 ± 48	310	Box area fluctuation (CHARMM36)	[56]
		457 ± 9	310	Box area fluctuation (MARTINI v2.2)	
	65:35	686 ± 7	298	Box area fluctuation (Berger lipids)	Present work
POPC:ChoL	70:30	673	298	Micropipette aspiration	[57]

obtained by Evans et al. for the same composition using micropipette aspiration [57]. Saeedimasine et al. reported lower values [56], easily explained by the difference in temperature (298 K in our case vs 310 K by Saeedimasine et al.).

We then calculated the compressibility modulus in the presence of increasing amounts of quercetin. We found that K_A decreases with increasing quercetin concentration, approximately in a linear fashion.

The trend is in qualitative agreement with the experimental results by AFM, indicating that quercetin softens lipid bilayers. A quantitative comparison is problematic, due to differences in cholesterol concentration in the samples used for AFM experiments.

Liposome softening is relevant in the context of drug delivery. The precise effect of liposome rigidity on the drug delivery process is still debated, but data is available on different drug delivery vectors. For instance, in vitro experiments on SUM159 cancer cells showed that softer (TA/PVPON) spherical particles are internalized more efficiently than their more rigid counterparts [58]. Hartmann et al. showed that softer (DextS/PLArg) and colloidal (PSS/PAH) particles were internalized and transported to lysosomes faster than more rigid particles in HeLa cells [59]. In the case of lipid vesicles, it is not clear whether their rigidity has an effect on internalization and intra-cellular transport. Sun et al. synthetized lipid-covered polymeric nanoparticles (NPs) and varied water content and rigidity but with the same chemical composition, size, and surface properties [60]. They show that nanoparticles with a rigid lipid shell enter cells more easily than softer ones. Cellular uptake was tested by incubating the vesicles with HELA cells and human umbilical vein endothelial cells (HUVECs). Also, using MD simulations the authors showed that the soft NPs were deformed and thus energetically unfavorable for cellular uptake [60]. Yu et al. demonstrated, via both molecular-dynamics simulations and super-resolution microscopy, that liposomes with moderate rigidity displayed enhanced diffusivity through mucus and thus achieved an oral insulin delivery efficacy superior to that of both their soft and hard counterparts [61]. Also, they showed that liposomes with different transition temperatures (T_m) have different rigidities and further transform into various shapes, which results in different diffusion coefficients.

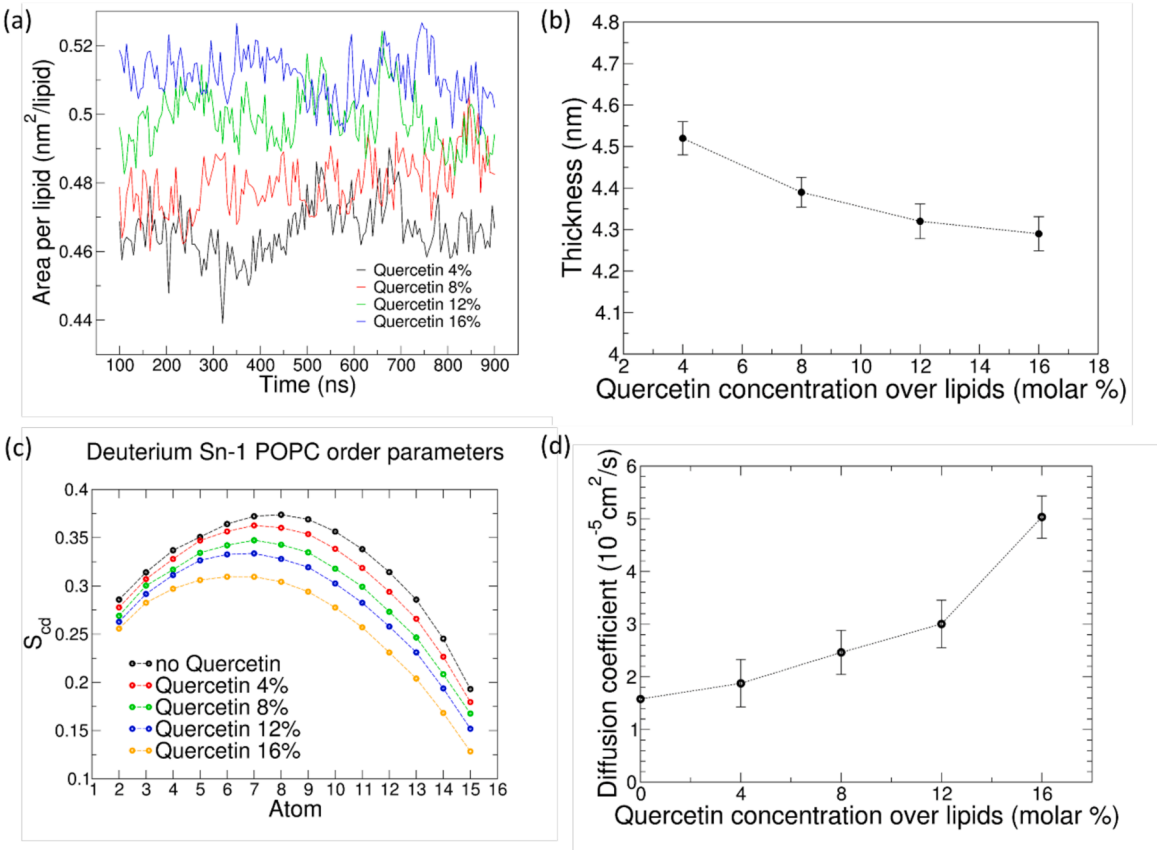

Fig. 5. Variation of structural parameters of lipid membranes. (a). Area per lipid; (b) membrane thickness; (c) deuterium order parameter of sn-1 chain of POPC, and (d) diffusion coefficient of POPC lipids.

In order to interpret the membrane softening effect in terms of molecular interactions, we analyzed how quercetin affects membrane structural and dynamic properties, namely thickness, area per lipid, deuterium order parameter of sn-1 acyl chain of POPC lipids, and POPC diffusion coefficients (Fig. 5).

We found that the area per lipid increases with quercetin concentration. The estimate does not take into account the fraction of membrane area taken by quercetin. On the other hand, the average value of bilayer thickness decreases with increasing quercetin concentration. This is consistent with a decrease in the order parameter for POPC acyl chains (Fig. 5c). Also, the diffusion coefficient of POPC lipids increases in the presence of quercetin molecules, from 1.58 $10^{-5} cm^2/s$ in the absence of quercetin to 5.03 $10^{-5} cm^2/s$ in membranes containing 16% quercetin. The overall picture is very consistent: in the presence of quercetin, membranes get thinner and more disordered, hence softer; more space is available to each lipid, which increases their diffusion rates. Similar findings were obtained by Sanver et al. using X-ray scattering after encapsulating quercetin in DOPC membranes [62]: in their report it was shown that the presence of quercetin reduces bilayer thickness and increases bilayer undulations, leading to a membrane-fluidizing effect.

How can such softening effect be interpreted in terms of molecular interactions? We can use the same MD simulations to determine the interaction of quercetin with the lipids at the atomistic level. First, we verified by visual inspection that, even at the highest concentration, quercetin does not aggregate inside the bilayer (see Fig. 6). Then, we determined the position and orientation of quercetin in the membrane by calculating the symmetrized partial densities of quercetin molecules. We then calculated the distribution of the angle between the bilayer normal and the plane of the larger aromatic ring (Fig. 7), defined by atoms 6-8-13 (see Fig. 1).

Partial density profiles indicate that quercetin is preferentially located below the lipid head group region, at the interface between the highly hydrated glycerol groups and the apolar acyl chains, at all concentrations. The preferred orientation of quercetin is with the aromatic rings in the plane containing the bilayer normal (Fig. 7a). The vector defined by atoms C13 and C16 (see Fig. 1), crossing the larger aromatic ring, is preferentially tilted with respect to the bilayer normal (Fig. 7b). Fluctuations in the molecular orientation are broad, but overall the orientation of aromatic rings allows atoms O29 and O26 (hydroxyl groups in the phenyl ring) to be in the proximity of the water interface, as confirmed by the average numbers of hydrogens bonds with water molecules (3.4 $\pm$ 1 hydrogen bonds per quercetin molecule on average, data not shown). The larger aromatic ring is embedded more deeply in the membrane compared to the smaller (phenyl) ring. Simulations also allow us to be more precise, and study the most favorable contacts within the membrane. For instance, atom C13 makes contact mostly with the first carbon atom of sn-1 chains (90 $\pm$ 4 % contact fraction, while the fraction of phospholipids in the system is only 65%), while contacts with the last carbon atom of acyl chains are infrequent (35$\pm$ 20 %); this is consistent with partial density profiles (Fig. 6) and also suggests that quercetin is more often in contact with phospholipids than it is with cholesterol. Overall, the localization of quercetin agrees well with previous data obtained by electron paramagnetic resonance (EPR) measurements on DPPC (1,2-dipalmitoyl-snglycero- 3-phosphocholine) liposomes, and is consistent with fluorescence spectroscopy data on human skin fibroblast cells [16]. It is also compatible with MD simulations by Kosinova et al. [30], Fabre et al. [63], and by Sanver et al. [62], showing that quercetin localizes below the polar region of the membrane. We notice that the orientation of the aromatic rings reported by previous simulations is almost parallel to the membrane surface. This is different from our findings. However, the lipid composition used in previous studies is different (DOPC, while we used a POPC+POPE+CHOL mixture), and differences in the force fields can also contribute to differences in orientation; in particular, we notice that the partial charges for all oxygen atoms are higher in both Kosinova et al. [30] and Sanver et al. [62], which makes it more favorable for the molecule to be in contact with water – hence the preferential localization on the membrane surface.

To better understand how quercetin localization affects lipid-lipid interactions, we calculated the 2D radial distribution function *g(r)* for the center of mass (COM) of lipid molecules, and for the COM of lipid acyl chains (Fig. 8). It is apparent that, with increasing quercetin concentrations, larger distances between the lipid molecules are more frequently sampled; in other words, lipid molecules are more frequently found farther apart from one another. This is due to the presence of the flavonoid, intercalating among lipid acyl chains. Looser packing of acyl chains is also demonstrated by lower order parameters, as reported above, and by lower lipid-lipid interaction energies (Fig. 8c), and appears to be correlated with membrane softening by quercetin.

Previous studies have reported effects of flavonoids on membrane properties. For example, Ingólfsson et al. examined the membrane localization and bilayer-modifying effects of five phenolic phytochemicals—capsaicin, curcumin, epigallocatechin gallate, genistein, and resveratrol [64]. The authors used MD simulations using both Martini and all-atom force fields and found that phytochemicals localize into the bilayer/solution interface of POPC membrane (lipid headgroup and backbone region). The simulations showed that those phytochemicals have modest effects on the bilayer structural properties (increases in the average area per lipid or decreases in bilayer thickness) with little effect on average lipid order or bilayer compressibility, but they produced significant changes in the bilayer pressure profile – and hence on elastic properties [64]. Huh et al. used X-ray diffraction and NMR to show that tannic acids, naturally occurring polyphenolic compounds, also weaken bilayer integrity through an increase in membrane area [65]. Tamba et al. demonstrated (using both phase-contrast fluorescence microscopy and the single GUV method) that tea catechins, which are flavonoids, disrupt bilayers, rupture lipid vesicles, and induce cell lysis [66]. Sanver et al. studied the effect of quercetin and rutin on DOPC membrane structural parameters using both X-ray diffraction and MD simulations [62]. They showed that both molecules partitioned within lipid bilayers (at different locations), increased the lattice spacing, reduced bilayer thickness, and increased bilayer undulations. The influence of rutin was not as strong as for quercetin, due to the different location of both molecules in the membrane; quercetin is located more deeply in the membrane. Gharib *et al.* studied the interaction of DPPC bilayer membranes with a series of monoterpenes including eucalyptol, pulegone, α-terpineol, β-terpineol, γ-terpineol, δ-terpineol and thymol, using differential scanning calorimetry, Raman spectroscopy and fluorescence anisotropy [67]. They showed that monoterpens abolished the pre-transition of DPPC membrane and modified the intensity of the Raman peaks. The molecules also decreased the main transition temperature of DPPC bilayers, suggesting their interaction with the alkyl chains of DPPC membrane. Fluorescence anisotropy results suggested that monoterpenes fluidized the liposomal membrane at 25, 41, and 50°C. Kaddah *et al.*, investigated the impact of a series of glucocorticoids molecules with different concentrations on the membrane fluidity of DPPC liposomes using electron paramagnetic resonance spectroscopy measurement [67]. They showed that the molecules concentration is a key parameter that affect the membrane fluidity of DPPC liposomes.

The relevance of our findings is threefold. First of all, softening of liposomes is relevant in the context of drug delivery, as shown in numerous previous studies. Indeed, membrane rigidity can dramatically alter cellular uptake efficiency for lipid-coated drug delivery vectors [17,60]. Second, softening of model membranes by quercetin indicates that probably a similar effect would be observed also in cell membranes, if sufficiently high concentrations of the flavonoid are (locally) reached. A recent study showed that membrane elasticity correlates with lipid ordering and viscosity in cells [68] – in agreement with our observations in model systems. Third, membrane softening and membrane thinning can have important effects on the activity of membrane proteins, as

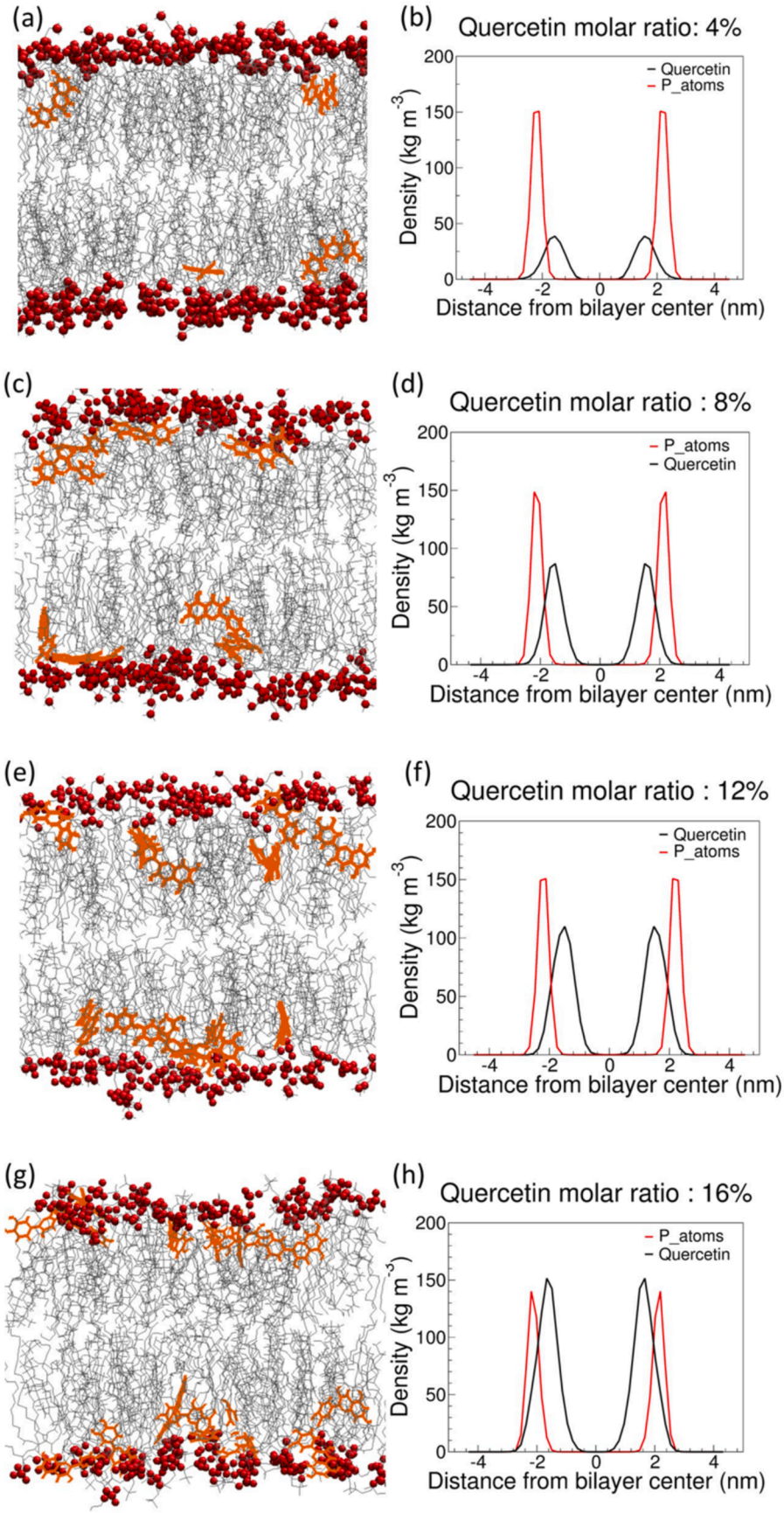

Fig. 6. (a–h) Snapshots (left panels) and partial density profiles (right panels) of quercetin in membranes at different concentrations. Lipid head groups are in red, acyl chains in gray, and quercetin in orange. The partial density of phosphorus atoms in lipid head groups is reported for reference.

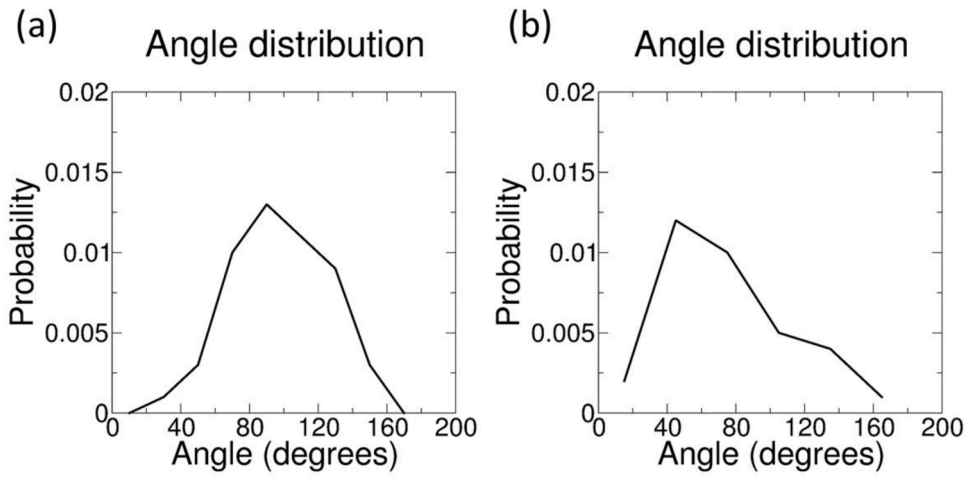

Fig. 7. (a) Quercetin orientation in the membrane, quantified as angle distribution; the angle is defined by the bilayer normal (z-axis) and the normal to the larger aromatic ring (defined by atoms C6, C8 and C13 of quercetin, see Fig. 1). (b) Quercetin orientation in the membrane, quantified as the angle between the C13-C6 vector and the bilayer normal (z axis).

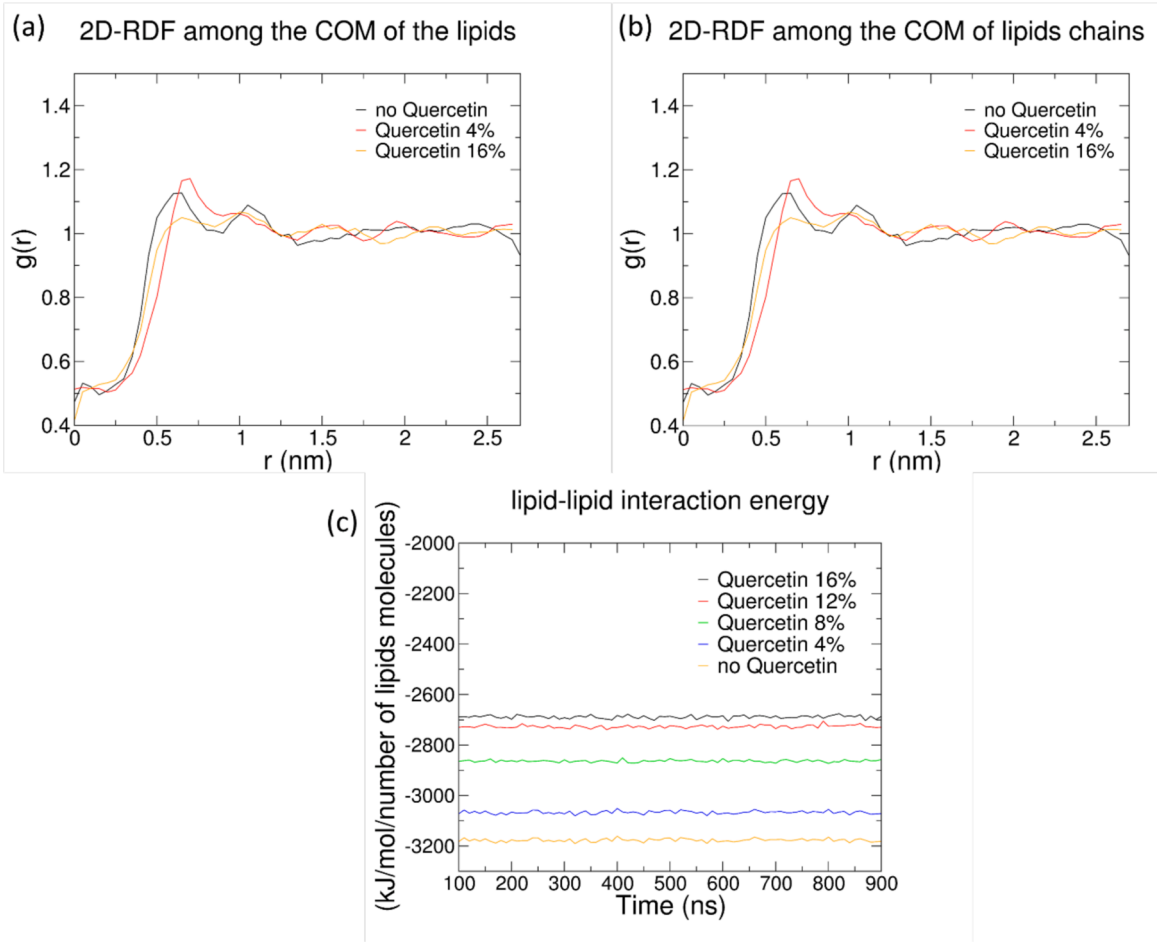

Fig. 8. Variation of 2D radial distribution functions as a function of quercetin concentration; (a) Center of mass (COM) of lipid molecules, and (b) COM of lipids tails. Only three compositions are reported, for the sake of clarity. (c) Lipid-lipid interaction energy in simulations with different concentration of quercetin.

reported in a number of studies (for reviews, see [69–71]). For a protein in which the hydrophobic length of the active state is longer than that of the inactive state, the protein activity will increase when the average bilayer thickness increases (within a given range), and vice versa [69, 70]. Also, softening the bilayer may shift the conformational equilibrium toward the state with higher hydrophobic mismatch [69,70]. Hence, bilayer softening could increase or decrease protein activity depending on the specific protein–bilayer structural and elastic properties. This is corroborated by the observation that lipid chain length is often found to modulate the function of integral membrane proteins; in numerous cases, the enzyme or transport activity reaches a maximum at a particular lipid chain length and is reduced in membranes with either

shorter or longer lipid chains [70].

Conclusions

In this work, we investigated the effect of quercetin on the bending rigidity of lipid membranes using AFM measures and MD simulations. AFM data show that the average values of Young modulus decrease in the presence of quercetin, but the decrease is difficult to interpret due to the different cholesterol content of the quercetin-loaded liposomes, and the relatively large statistical uncertainty of the AFM measures. Atomistic MD simulations confirm that quercetin softens the bilayer membrane, and also indicate that it decreases membrane thickness and increases disorder of acyl chains. Consistent with such changes in structural properties, diffusion coefficients are also increased. Changes in structural and dynamic properties can be interpreted in the light of quercetin localization and orientation in the membrane: due to its amphipathic nature, quercetin is located preferentially at the interface between the hydrophobic core and polar head groups of the lipids, roughly parallel to the membrane normal; in such position and orientation, quercetin increases the average distance among phospholipids, reducing their mutual attraction and softening the membrane. Membrane softening and thinning have been found before to be relevant in the context of drug delivery vehicles, as well as for their potential effects on biological functions.

Declaration of Competing Interest

The authors declare that they have no known competing financial interests or personal relationships that could have appeared to influence the work reported in this paper.

Acknowledgement

LM acknowledges funding from the *Institut National de la Sante et de la Recherche Medical* (INSERM). Calculations were performed in part at the French supercomputing center CINES, supported by *Grand Equipement National de Calcul Intensif* (GENCI, grant number A0080710138). JE acknowledges funding from the *Association de coopération, développement et santé of Lebanon*.

Supplementary materials

Supplementary material associated with this article can be found, in the online version, at doi:10.1016/j.bbadva.2021.100018.

References

[1] A.T. Jan, M.R. Kamli, I. Murtaza, J.B. Singh, A. Ali, Q.M.R. Haq, Dietary flavonoid quercetin and associated health benefits—an overview, Food Rev. Int. 26 (2010) 302–317.
[2] A.W. Boots, G.R.M.M. Haenen, A. Bast, Health effects of quercetin: from antioxidant to nutraceutical, Eur. J. Pharmacol. 585 (2008) 325–337.
[3] K. Zandi, B.-T. Teoh, S.-S. Sam, P.-F. Wong, M.R. Mustafa, S. AbuBakar, Antiviral activity of four types of bioflavonoid against dengue virus type-2, Virol. J. 8 (2011) 560.
[4] J.G.A. Coelho-dos-Reis, O.A. Gomes, D.E. Bortolini, M.L. Martins, M.R. Almeida, C. S. Martins, L.D. Carvalho, J.G. Souza, J.M.C. Vilela, M.S. Andrade, E.F. Barbosa-Stancioli, Evaluation of the effects of quercetin and kaempherol on the surface of MT-2 cells visualized by atomic force microscopy, J. Virol. Methods 174 (2011) 47–52.
[5] F. Dajas, Life or death: neuroprotective and anticancer effects of quercetin, J. Ethnopharmacol. 143 (2012) 383–396.
[6] S. Andrés, M.L. Tejido, R. Bodas, L. Morán, N. Prieto, C. Blanco, F.J. Giráldez, Quercetin dietary supplementation of fattening lambs at 0.2% rate reduces discolouration and microbial growth in meat during refrigerated storage, Meat Sci. 93 (2013) 207–212.
[7] D. Wu, Y. Kong, C. Han, J. Chen, L. Hu, H. Jiang, X. Shen, d-Alanine:d-alanine ligase as a new target for the flavonoids quercetin and apigenin, Int. J. Antimicrob. Agents 32 (2008) 421–426.
[8] C.-F. Lin, Y.-L. Leu, S.A. Al-Suwayeh, M.-C. Ku, T.-L. Hwang, J.-Y. Fang, Anti-inflammatory activity and percutaneous absorption of quercetin and its polymethoxylated compound and glycosides: the relationships to chemical structures, Eur. J. Pharm. Sci. 47 (2012) 857–864.
[9] K.C.B. De Souza, V.L. Bassani, E.E.S. Schapoval, Influence of excipients and technological process on anti-inflammatory activity of quercetin and *Achyrocline satureioides* (Lam.) D.C. extracts by oral route, Phytomedicine 14 (2007) 102–108.
[10] S.F. Nabavi, G.L. Russo, M. Daglia, S.M. Nabavi, Role of quercetin as an alternative for obesity treatment: you are what you eat!, Food Chem. 179 (2015) 305–310.
[11] N.P. Aditya, A.S. Macedo, S. Doktorovova, E.B. Souto, S. Kim, P.-S. Chang, S. Ko, Development and evaluation of lipid nanocarriers for quercetin delivery: a comparative study of solid lipid nanoparticles (SLN), nanostructured lipid carriers (NLC), and lipid nanoemulsions (LNE), LWT - Food Sci. Technol. 59 (2014) 115–121.
[12] X. Cai, Z. Fang, J. Dou, A. Yu, G. Zhai, Bioavailability of quercetin: problems and promises, Curr. Med. Chem. 20 (2013) 2572–2582.
[13] J. Hao, B. Guo, S. Yu, W. Zhang, D. Zhang, J. Wang, Y. Wang, Encapsulation of the flavonoid quercetin with chitosan-coated nano-liposomes, LWT - Food Sci. Technol. 85 (2017) 37–44.
[14] F. Tamjidi, M. Shahedi, J. Varshosaz, A. Nasirpour, Nanostructured lipid carriers (NLC): a potential delivery system for bioactive food molecules, Innov. Food Sci. Emerg. Technol. 19 (2013) 29–43.
[15] T. Toniazzo, M.S. Peres, A.P. Ramos, S.C. Pinho, Encapsulation of quercetin in liposomes by ethanol injection and physicochemical characterization of dispersions and lyophilized vesicles, Food Biosci. 19 (2017) 17–25.
[16] B. Pawlikowska-Pawlęga, W. Ignacy Gruszecki, L. Misiak, R. Paduch, T. Piersiak, B. Zarzyka, J. Pawelec, A. Gawron, Modification of membranes by quercetin, a naturally occurring flavonoid, via its incorporation in the polar head group, Biochim. Biophys. Acta 1768 (2007) 2195–2204.
[17] A.C. Anselmo, S. Mitragotri, Impact of particle elasticity on particle-based drug delivery systems, Adv. Drug Del. Rev. 108 (2017) 51–67.
[18] J. Azzi, A. Jraij, L. Auezova, S. Fourmentin, H. Greige-Gerges, Novel findings for quercetin encapsulation and preservation with cyclodextrins, liposomes, and drug-in-cyclodextrin-in-liposomes, Food Hydrocolloids 81 (2018) 328–340.
[19] M.-L. Briuglia, C. Rotella, A. McFarlane, D.A. Lamprou, Influence of cholesterol on liposome stability and on in vitro drug release, Drug Deliv. Transl. Res. 5 (2015) 231–242.
[20] Y. Takechi-Haraya, K. Sakai-Kato, Y. Goda, Membrane rigidity determined by atomic force microscopy is a parameter of the permeability of liposomal membranes to the hydrophilic compound calcein, AAPS PharmSciTech 18 (2017) 1887–1893.
[21] A.M. Kloxin, J.A. Benton, K.S. Anseth, In situ elasticity modulation with dynamic substrates to direct cell phenotype, Biomaterials 31 (2010) 1–8.
[22] M. Frenzel, A. Steffen-Heins, Impact of quercetin and fish oil encapsulation on bilayer membrane and oxidation stability of liposomes, Food Chem. 185 (2015) 48–57.
[23] M. Huang, E. Su, F. Zheng, C. Tan, Encapsulation of flavonoids in liposomal delivery systems: the case of quercetin, kaempferol and luteolin, Food Funct. 8 (2017) 3198–3208.
[24] W. Phachonpai, J. Wattanathorn, S. Muchimapura, T. Tong-Un, D. Preechagoon, Neuroprotective effect of quercetin encapsulated liposomes: a novel therapeutic strategy against Alzheimer's disease, Am. J. Appl. Sci. 7 (2010) 480–485.
[25] O. Et-Thakafy, N. Delorme, C. Gaillard, C. Mériadec, F. Artzner, C. Lopez, F. Guyomarc'h, Mechanical properties of membranes composed of gel-phase or fluid-phase phospholipids probed on liposomes by atomic force spectroscopy, Langmuir 33 (2017) 5117–5126.
[26] X. Liang, G. Mao, K.Y. Simon Ng, Probing small unilamellar EggPC vesicles on mica surface by atomic force microscopy, Colloids Surf. B. Biointerfaces 34 (2004) 41–51.
[27] R.W. Storrs, F.D. Tropper, H.Y. Li, C.K. Song, J.K. Kuniyoshi, D.A. Sipkins, K.C. P. Li, M.D. Bednarski, Paramagnetic polymerized liposomes: synthesis, characterization, and applications for magnetic resonance imaging, J. Am. Chem. Soc. 117 (1995) 7301–7306.
[28] J. Eid, H. Greige-Gerges, L. Monticelli, A. Jraij, Elastic moduli of lipid membranes: reproducibility of AFM measures, Chem. Phys. Lipids 234 (2021), 105011.
[29] A. de Granada-Flor, C. Sousa, H.A.L. Filipe, M.S.C.S. Santos, R.F.M. de Almeida, Quercetin dual interaction at the membrane level, Chem. Commun. 55 (2019) 1750–1753.
[30] P. Košinová, K. Berka, M. Wykes, M. Otyepka, P. Trouillas, Positioning of antioxidant quercetin and its metabolites in lipid bilayer membranes: implication for their lipid-peroxidation inhibition, J. Phys. Chem. B 116 (2012) 1309–1318.
[31] R. Sinha, M. Gadhwal, U. Joshi, S. Srivastava, G. Govil, a. Nmr, T. Research, India Mumbai, b. Pharmacy, C. Parade, Interaction of quercetin with DPPC model membrane: molecular dynamic simulation, DSC and multinuclear NMR studies, J.-Indian Chem. Soc. 88 (2011) 1203–1210.
[32] E. Reissner, Stresses and small displacements of shallow spherical shells. II, J. Math. Phys. 25 (1946) 279–300.
[33] J.D. Berry, S. Mettu, R.R. Dagastine, Precise measurements of capsule mechanical properties using indentation, Soft Matter 13 (2017) 1943–1947.
[34] E.A. Evans, Bending resistance and chemically induced moments in membrane bilayers, Biophys. J. 14 (1974) 923–931.
[35] L.S. Dodda, I. Cabeza de Vaca, J. Tirado-Rives, W.L. Jorgensen, LigParGen web server: an automatic OPLS-AA parameter generator for organic ligands, Nucl. Acids Res. 45 (2017) W331–W336.
[36] L.S. Dodda, J.Z. Vilseck, J. Tirado-Rives, W.L. Jorgensen, 1.14*CM1A-LBCC: localized bond-charge corrected CM1A charges for condensed-phase simulations, J. Phys. Chem. B 121 (2017) 3864–3870.

[37] W.L. Jorgensen, J. Tirado-Rives, Potential energy functions for atomic-level simulations of water and organic and biomolecular systems, Proc. Natl. Acad. Sci. USA 102 (2005) 6665.
[38] G.A. Kaminski, R.A. Friesner, J. Tirado-Rives, W.L. Jorgensen, Evaluation and reparametrization of the OPLS-AA force field for proteins via comparison with accurate quantum chemical calculations on peptides, J. Phys. Chem. B 105 (2001) 6474–6487.
[39] M.J. Abraham, T. Murtola, R. Schulz, S. Páll, J.C. Smith, B. Hess, E. Lindahl, GROMACS: high performance molecular simulations through multi-level parallelism from laptops to supercomputers, SoftwareX 1-2 (2015) 19–25.
[40] K. Lemańska, H. van der Woude, H. Szymusiak, M.G. Boersma, A. Gliszczyńska-Świgło, I.M.C.M. Rietjens, B. Tyrakowska, The effect of catechol o-methylation on radical scavenging characteristics of quercetin and luteolin—a mechanistic insight, Free Radical Res. 38 (2004) 639–647.
[41] H.J.C. Berendsen, J.P.M. Postma, W.F. van Gunsteren, J. Hermans, Interaction models for water in relation to protein hydration, in: B. Pullman (Ed.), Intermolecular Forces, D. Reidel, Dordrecht, The Netherlands, 1981, pp. 331–342.
[42] C.J. Knight, J.S. Hub, MemGen: a general web server for the setup of lipid membrane simulation systems, Bioinformatics 31 (2015) 2897–2899.
[43] O. Berger, O. Edholm, F. Jahnig, Molecular dynamics simulations of a fluid bilayer of dipalmitoylphosphatidylcholine at full hydration, constant pressure, and constant temperature, Biophys. J. 72 (1997) 2002–2013.
[44] D.P. Tieleman, J.L. MacCallum, W.L. Ash, C. Kandt, Z.T. Xu, L. Monticelli, Membrane protein simulations with a united-atom lipid and all-atom protein model: lipid-protein interactions, side chain transfer free energies and model proteins, J. Phys.-Condens. Matter 18 (2006) S1221–S1234.
[45] J.L. MacCallum, W.F.D. Bennett, D.P. Tieleman, Distribution of amino acids in a lipid bilayer from computer simulations, Biophys. J. 94 (2008) 3393–3404.
[46] M. Paloncýová, R. DeVane, B. Murch, K. Berka, M. Otyepka, Amphiphilic drug-like molecules accumulate in a membrane below the head group region, J. Phys. Chem. B 118 (2014) 1030–1039.
[47] T. Darden, D. York, L. Pedersen, Particle mesh Ewald: an N-log(N) method for Ewald sums in large systems, J. Chem. Phys. 98 (1993) 10089–10092.
[48] U. Essmann, L. Perera, M.L. Berkowitz, T. Darden, H. Lee, L.G. Pedersen, A smooth particle mesh Ewald potential, J. Chem. Phys. 103 (1995) 8577–8592.
[49] B. Hess, P-LINCS: a parallel linear constraint solver for molecular simulation, J. Chem. Theory Comput. 4 (2008) 116–122.
[50] G. Bussi, D. Donadio, M. Parrinello, Canonical sampling through velocity rescaling, J. Chem. Phys. 126 (2007), 014101.
[51] H.J.C. Berendsen, J.P.M. Postma, W.F. van Gunsteren, A. di Nola, J.R. Haak, Molecular dynamics with coupling to an external bath, J. Chem. Phys. 81 (1984) 3684–3690.
[52] M. Parrinello, A. Rahman, Polymorphic transitions in single crystals - a new molecular dynamics method, J. Appl. Phys. 52 (1981) 7182–7190.
[53] Y. Takechi-Haraya, K. Sakai-Kato, Y. Abe, T. Kawanishi, H. Okuda, Y. Goda, Atomic force microscopic analysis of the effect of lipid composition on liposome membrane rigidity, Langmuir 32 (2016) 6074–6082.
[54] J. Eid, H. Razmazma, A. Jraij, A. Ebrahimi, L. Monticelli, On calculating the bending modulus of lipid bilayer membranes from buckling simulations, J. Phys. Chem. B 124 (2020) 6299–6311.
[55] M. Doktorova, M.V. LeVine, G. Khelashvili, H. Weinstein, A new computational method for membrane compressibility: bilayer mechanical thickness revisited, Biophys. J. 116 (2019) 487–502.
[56] M. Saeedimasine, A. Montanino, S. Kleiven, A. Villa, Role of lipid composition on the structural and mechanical features of axonal membranes: a molecular simulation study, Sci. Rep. 9 (2019) 8000.
[57] E. Evans, W. Rawicz, B.A. Smith, Concluding remarks Back to the future: mechanics and thermodynamics of lipid biomembranes, Faraday Discuss 161 (2013) 591–611.
[58] J.F. Alexander, V. Kozlovskaya, J. Chen, T. Kuncewicz, E. Kharlampieva, B. Godin, Cubical shape enhances the interaction of layer-by-layer polymeric particles with breast cancer cells, Adv. Healthc. Mater. 4 (2015) 2657–2666.
[59] R. Hartmann, M. Weidenbach, M. Neubauer, A. Fery, W.J. Parak, Stiffness-dependent in vitro uptake and lysosomal acidification of colloidal particles, Angew. Chem. Int. Ed. 54 (2015) 1365–1368.
[60] J. Sun, L. Zhang, J. Wang, Q. Feng, D. Liu, Q. Yin, D. Xu, Y. Wei, B. Ding, X. Shi, X. Jiang, Tunable rigidity of (polymeric core)–(lipid shell) nanoparticles for regulated cellular uptake, Adv. Mater. 27 (2015) 1402–1407.
[61] M. Yu, W. Song, F. Tian, Z. Dai, Q. Zhu, E. Ahmad, S. Guo, C. Zhu, H. Zhong, Y. Yuan, T. Zhang, X. Yi, X. Shi, Y. Gan, H. Gao, Temperature- and rigidity-mediated rapid transport of lipid nanovesicles in hydrogels, Proc. Natl. Acad. Sci 116 (2019) 5362. USA.
[62] D. Sanver, A. Sadeghpour, M. Rappolt, F. Di Meo, P. Trouillas, Structure and dynamics of dioleoyl-phosphatidylcholine bilayers under the influence of quercetin and rutin, Langmuir 36 (2020) 11776–11786.
[63] G. Fabre, I. Bayach, K. Berka, M. Paloncýová, M. Starok, C. Rossi, J.-L. Duroux, M. Otyepka, P. Trouillas, Synergism of antioxidant action of vitamins E, C and quercetin is related to formation of molecular associations in biomembranes, Chem. Commun. 51 (2015) 7713–7716.
[64] H.I. Ingólfsson, P. Thakur, K.F. Herold, E.A. Hobart, N.B. Ramsey, X. Periole, D. H. de Jong, M. Zwama, D. Yilmaz, K. Hall, T. Maretzky, H.C. Hemmings, C. Blobel, S.J. Marrink, A. Koçer, J.T. Sack, O.S. Andersen, Phytochemicals perturb membranes and promiscuously alter protein function, ACS Chem. Biol. 9 (2014) 1788–1798.
[65] N.W. Huh, N.A. Porter, T.J. McIntosh, S.A. Simon, The interaction of polyphenols with bilayers: conditions for increasing bilayer adhesion, Biophys. J. 71 (1996) 3261–3277.
[66] Y. Tamba, S. Ohba, M. Kubota, H. Yoshioka, H. Yoshioka, M. Yamazaki, Single GUV method reveals interaction of tea catechin (−)-epigallocatechin gallate with lipid membranes, Biophys. J. 92 (2007) 3178–3194.
[67] S. Kaddah, N. Khreich, F. Kaddah, L. Khrouz, C. Charcosset, H. Greige-Gerges, Corticoids modulate liposome membrane fluidity and permeability depending on membrane composition and experimental protocol design, Biochimie 153 (2018) 33–45.
[68] J. Steinkühler, E. Sezgin, I. Urbančič, C. Eggeling, R. Dimova, Mechanical properties of plasma membrane vesicles correlate with lipid order, viscosity and cell density, Commun. Biol. 2 (2019) 337.
[69] O.S. Andersen, R.E. Koeppe, Bilayer thickness and membrane protein function: an energetic perspective, Annu. Rev. Biophys. Biomol. Struct. 36 (2007) 107–130.
[70] D. Marsh, Protein modulation of lipids, and vice-versa, in membranes, Biochim. Biophys. Acta (2008) 1545–1575, 1778.
[71] T.J. McIntosh, S.A. Simon, Roles of bilayer material properties in function and distribution of membrane proteins, Annu. Rev. Biophys. Biomol. Struct. 35 (2006) 177–198.